

Published in Nature Photonics, vol.2, no.12, pp.728-732 (2008). (First version)

Fast physical random bit generation with chaotic semiconductor lasers

Atsushi Uchida^{1,2),*}, Kazuya Amano¹⁾, Masaki Inoue¹⁾, Kunihito Hirano¹⁾, Sunao Naito¹⁾,
Hiroyuki Someya¹⁾, Isao Oowada¹⁾, Takayuki Kurashige¹⁾, Masaru Shiki¹⁾,
Shigeru Yoshimori¹⁾, Kazuyuki Yoshimura³⁾, and Peter Davis³⁾

¹⁾ Department of Electronics and Computer Systems, Takushoku University,
815-1 Tatemachi, Hachioji, Tokyo 193-0985, Japan

²⁾ Department of Information and Computer Sciences, Saitama University,
255 Shimo-Okubo, Sakura-ku, Saitama city, Saitama, 338-8570, Japan

³⁾ NTT Communication Science Laboratories, NTT Corporation,
2-4 Hikaridai, Seika-cho, Soraku-gun, Kyoto, 619-0237 Japan

* Corresponding author:

Department of Information and Computer Sciences, Saitama University
255 Shimo-Okubo, Sakura-ku, Saitama city, Saitama, 338-8570, Japan

Tel: +81-48-858-3490

Fax: +81-48-858-3716

Email: auchida@mail.saitama-u.ac.jp

laserchaos@hotmail.com

Random number generators in digital information systems exploit physical entropy sources, such as electronic and photonic noise, to add unpredictability to deterministically generated pseudo-random sequences [1, 2]. However, there is a large gap between the generation rates achieved with existing physical sources and the high data rates of many computation and communication systems, which is a fundamental weakness in these systems. Here we show that good-quality random bit sequences can be generated at very fast bit rates using physical chaos in semiconductor lasers. Streams of bits which pass standard statistical tests for randomness have been generated at rates of up to 1.7 gigabit per second by sampling the fluctuating optical output of two chaotic lasers. This rate is an order of magnitude faster than that of previously reported devices for physical random bit generators with verified randomness. This means that the reliability of random numbers in high performance systems can be greatly improved by using chaotic laser devices as physical entropy sources.

The performance and reliability of our digital networked society relies on the ability to generate large quantities of randomness. For example, random numbers are commonly used in computations to solve problems in nuclear medicine, computer graphics, finance, biophysics, computational chemistry, and materials science [3]. Also, random numbers are used in transactions on the internet to ensure confidentiality (encryption), authentication (challenge-response protocols) and data integrity (digital signatures) [1,2]. Future deployments of quantum cryptography systems will require the generation of trusted random numbers to select photon detection parameters [4]. Accompanying the growing reliance on random numbers, there are earnest efforts to establish standards for random number generation based on stringent tests of

randomness [5-7].

Random numbers can be generated using physical processes. For example, physical randomizing devices based on “chaotic” physical phenomena, such as dice, shuffling playing cards, and roulette wheels, have long been used for games and gambling as well as scientific purposes [8]. Later, methods were developed to generate many pseudo-random numbers from a single random “seed” using deterministic algorithms, and these are used in modern digital electronic information systems [9]. However, sequences of pseudo-random numbers generated deterministically from the same seed will be identical, and this can cause serious problems for applications in security or parallel computation systems. Truly random numbers should be un-predictable, un-reproducible, and statistically unbiased. For this reason, physically random processes are often used as entropy sources in random number generators [10,11]. Random phenomena such as photon noise, thermal noise in resistors and frequency jitter of oscillators have been used as physical entropy sources for non-deterministic bit generation in combination with deterministic pseudo-random number generators [12-17]. However, non-deterministic generators have been limited to much slower rates than pseudo-random generators due to limitations of the rate and power of the mechanisms for extracting bits from physical noise.

In this letter, we report that we have succeeded in generating random bit sequences at a rate of more than one gigabit per second (Gbps) using high-bandwidth chaotic semiconductor lasers. Chaotic systems generate large amplitude random signals from microscopic noise by nonlinear amplification and mixing mechanisms [18-23]. We exploit chaos in lasers to achieve efficient and stable generation of random bits at high frequencies. High-bandwidth chaotic lasers have been previously used to demonstrate

transmission of messages hidden in complex optical waveforms [24-26]. However, this is the first time that chaotic lasers have been used to demonstrate high-rate generation of random bit sequences with verified randomness.

The structure of the scheme for generating random bit sequences using chaotic lasers is shown in Fig. 1a. The scheme uses two semiconductor lasers set-up to exhibit high-bandwidth chaotic intensity oscillations with different average frequency and autocorrelation characteristics. The output intensity of each laser is converted to an electrical signal by photo-detectors, amplified and converted to a binary signal using a 1-bit analog-digital converter (ADC) driven by a fast clock. The binary signals thus obtained from the two lasers are combined by a logical Exclusive-OR (XOR) operation to generate a single random bit sequence. No other digital post-processing is required.

An implementation of the scheme is shown in Fig. 1b. (see also Supplementary Fig. S1). Semiconductor lasers with external optical feedback [26-29] are used to generate optical chaos with high-bandwidth in the gigahertz regime. Single-mode distributed-feedback (DFB) lasers are modified to allow optical feedback from an external fiber reflector which reflects a fraction of the light back into the laser, inducing high-frequency chaotic oscillations. The ADC consists of a comparator and a D flip flop, which first converts the input analog signal into a binary level by comparing with a set threshold voltage, and then samples the binary level at the rising edge of an external clock.

The procedure for realizing random bit generation at a particular bit rate is as follows. First we adjust the injection current, the length of the external cavity and the external feedback strength to put the lasers in a regime of high bandwidth-chaos. Then the parameters of the two lasers are adjusted to “detune” their chaotic oscillations so

their largest oscillation components and the clock frequency are incommensurate, and correlations are small, as explained below. Then the threshold levels of the ADC are adjusted to equalize the ratio of 0 and 1 at the XOR output.

An example of random bit generation is shown in Fig. 2. The rate is 1.7 Gbit per second, corresponding to an external clock with frequency of 1.7 GHz. The temporal waveforms of the two chaotic outputs of the laser intensities, the external clock, and the physical random bits obtained from the electronic circuit are shown in Fig. 2a. The sampling of the chaotic signals by the ADCs is triggered by the rising edge of the external clock (see the solid dots on the chaotic temporal waveforms in Fig. 2a). The threshold values for the ADCs are shown as solid lines in Fig. 2a. The signal at the bottom of Fig. 2a is the sequence of random bits output from the XOR operation, in the format of Non-Return-to-Zero (NRZ) that is suitable for high-speed data communications. The eye diagram of the output NRZ signal is shown in Fig. 2b. A visualization of the randomness of the bits is shown in Fig. 2c by plotting a single bit sequence as a 500x500 pattern of black and white dots (see also Supplementary Video S1).

To evaluate the randomness of digital bit sequences we used the standard statistical test suite for random number generators provided by National Institute of Standard Technology (NIST) and the Diehard test suite [5-7]. The tests were performed using 1000 instances of 1 Mbit sequences for NIST tests and using 74 Mbit sequences for Diehard tests. Bit sequences obtained from the experiment passed all of the NIST and Diehard tests. Typical results of the NIST tests are shown in Table 1. (Diehard results are shown in Supplementary Fig. S2).

In order to generate bit sequences which have no detectable correlations and pass

the statistical tests, the chaotic oscillations are tuned with respect to the clock rate. Examples of the autocorrelation functions of the intensity fluctuations of the two lasers and of the corresponding random bit sequence are shown in Figs. 3a-3c. The largest correlation peaks correspond to the delay time of the optical feedback ($\tau_{1,2}$) and the largest chaotic oscillation component ($\tau_{c1,c2}$). The correlation peaks decay rapidly over a few periods due to the strongly chaotic dynamics. Given the clock sampling period τ_s , the laser chaos is adjusted to satisfy the following conditions: (i) $\tau_{1,2} > \tau_s > \tau_{c1,c2}$ (ii) $l\tau_1 \neq m\tau_2 \neq n\tau_s$ (l, m, n are simple integers) to ensure incommensurateness of the largest oscillation components and avoid sampling correlated parts of the waveforms.

The non-determinism (i.e., unpredictability) property of the bit sequences is assured by the amplification of microscopic laser noise by chaotic dynamics. This can be confirmed by numerical analysis of the theoretical Lang-Kobayashi model for semiconductor lasers with optical feedback [27,29]. Adding noise consistent with the experimental noise power (Fig. 3d), and considering 1-bit sampling, the predictability time is 1~2 ns (Supplementary Fig. S3). This corresponds to an average entropy rate of over 500 Mbps per laser, giving a combined entropy rate of over 1 Gbps for the two laser scheme. Simulations with smaller noise levels exhibit longer predictability times. In this sense, the intrinsic laser noise is important for achieving high entropy rates in this system.

We further confirmed that the intrinsic laser noise alone is not sufficient for fast random bit generation. Non-chaotic laser noise obtained using the same ADC system when the optical feedback is reduced to zero (Fig. 3d) results in sequences with biased ratios of 0 and 1 for all values of the ADC threshold voltages (Supplementary Fig. S4). This shows that the large amplitude chaotic laser oscillation induced by optical feedback

is more effective than non-chaotic laser noise for generating fast random bit sequences.

Finally, we note that random bit generation at even faster rates can be achieved by using schemes which enhance the bandwidth of the chaos in the lasers, such as optical injection [30]. We confirmed that sequences which passed both the NIST and Diehard randomness tests were obtainable at rates up to 6.2 Gbps using optical injection to enhance the bandwidth of chaos beyond 10 GHz. Design of laser schemes to achieve higher rates of 10 Gbps and more, and their integration in compact photonic modules is a promising direction for future study.

In conclusion, we have demonstrated that continuous streams of random bit sequences which pass standard tests of randomness are generated at fast rates of up to 1.7 Gbps by directly sampling the output of two chaotic semiconductor lasers. The rate that we obtained is faster than that of any previously reported devices for physical generation of bit sequences with verified randomness, and demonstrates the large potential for improvements in performance of random number generators by harnessing chaotic laser devices as physical entropy sources.

References

- [1] Eastlake, D., Schiller, J. & Crocker, S. Randomness requirements for security. RFC4086 (2005) <http://tools.ietf.org/html/rfc4086>
- [2] Security requirements for cryptographic modules. FIPS 140-2 (2001)
<http://csrc.nist.gov/publications/fips/fips140-2/fips1402.pdf>
- [3] Metropolis, N. & Ulam, S. The Monte Carlo method. *Journal of the American Statistical Association* **44**, 335-341 (1949).
- [4] Gisin, N., Robordy, G, Tittel, W. & Zbinden, H. Quantum Cryptography. *Reviews of Modern Physics* **74**, 145-195 (2002).
- [5] Marsaglia, G. DIEHARD: A battery of tests of randomness. [http://stat.fsu.edu/ geo](http://stat.fsu.edu/geo), (1996).
- [6] Rukhin, A., Soto, J., Nechvatal, J., Smid, M., Barker, E., Leigh, S. & Levenson, M. A statistical test suite for random and pseudorandom number generators for cryptographic applications. *National Institute of Standards and Technology, Special Publication 800-22* (2001).
- [7] Kim, S. J., Umeno, K. & Hasegawa, A. Corrections of the NIST statistical test suite for randomness. *arXiv:nlin.CD/0401040v1* (2004).
- [8] Galton, F. Dice for statistical experiments. *Nature* **42**, 13-14 (1890).
- [9] Knuth, D. *The Art of Computer Programming: Volume 2: Seminumerical Algorithms (3rd Edition)* (Addison-Wesley Professional, 1996).
- [10] Kelsey, J. Entropy and entropy sources in X9.82. NIST (2004)
- [11] Schindler, W. & Killmann, W. Evaluation criteria for true (physical) random number generators used in cryptographic applications. *CHES 2002, Lecture Notes in Computer Science* **2523** 431–449 (Springer-Verlag, Berlin Heidelberg) (2002).

- [12] Jun, B. & Kocher, P. The Intel random number generator. *White Paper Prepared for Intel Corporation, Cryptography Research Inc.*, (1999).
<http://www.cryptography.com/resources/whitepapers/IntelRNG.pdf>.
- [13] Holman, W.T., Connelly, J.A. & Dowlatabadi, A.B. An integrated analog/digital random noise source. *IEEE Trans. Circuits and Systems I*, **44**, 521-528 (1997).
- [14] Stefanov, A., Gisin, N., Guinnard, O., Guinnard, L. & Zbinden, H. Optical quantum random number generator. *Journal of Modern Optics* **47**, 595-598 (2000).
- [15] Cortigiani, F., Petri, C., Rocchi, S. & Vignoli, V. Very high-speed true random noise generator. *The 7th IEEE International Conference on Electronics, Circuits and Systems, 2000 (ICECS 2000)* **1**, 120 - 123 (2000).
- [16] Bucci, M., Germani, L., Luzzi, R., Trifiletti, A. & Varanouvo, M. A high-speed oscillator-based truly random number source for cryptographic applications on a Smart Card IC. *IEEE Transactions on Computers* **52**, 403-409 (2003).
- [17] Tokunaga, C., Blaauw, D. & Mudge, T. True random number generator with a metastability-based quality control. *IEEE Journal of Solid-State Circuits* **43**, 78-85 (2008).
- [18] Ornstein, D. S. Ergodic theory, randomness, and "Chaos". *Science* **243** 182-187 (1989).
- [19] Wolfram, S. Random sequence generation by cellular automaton. *Advances in Applied Mathematics* **7**, 123-169 (1986).
- [20] Stojanovski, T. & Kocarev, L. Chaos-based random number generators-part I: analysis [cryptography]. *IEEE Transactions on Circuits and Systems I: Fundamental Theory and Applications*, **48**, 281-288 (2001).
- [21] Pappu, R., Recht, B., Taylor, J. & Gershenfeld, N. Physical one-way functions.

Science **297**, 2026-2030 (2002).

[22] Gleeson, J. T. Truly random number generator based on turbulent electroconvection. *Appl. Phys. Lett.* **81**, 1949 (2002).

[23] Callegari, S., Rovatti, R. & Setti, G. Embeddable ADC-based true random number generator for cryptographic applications using nonlinear signal processing and chaos. *IEEE Trans. Signal Processing* **53**, 793-805 (2005).

[24] VanWiggeren, G. D. & Roy, R. Communication with chaotic lasers. *Science*, **279**, 1198-1200 (1998).

[25] Argyris, A., Syvridis, D., Larger, L., Annovazzi-Lodi, V., Colet, P., Fischer, I., García-Ojalvo, J., Mirasso, C. R., Pesquera, L. & Shore, K. A. Chaos-based communications at high bit rates using commercial fibre-optic links. *Nature* **438**, 343-346 (2005).

[26] Liu, J. M., Chen, H. F. & Tang S. Synchronized chaotic optical communications at high bit rates. *IEEE Journal of Quantum Electronics* **38**, 1184- 1196 (2002).

[27] Lang, R. & Kobayashi, K. External optical feedback effects on semiconductor injection laser properties. *IEEE Journal Quantum Electronics* **16**, 347- 355 (1980).

[28] Kane, D. & Shore, K. A. (ed.) *Unlocking dynamical diversity: optical feedback effects on semiconductor lasers*. (John Wiley and Sons, Chichester, 2005).

[29] Uchida, A., Liu, Y. & Davis, P. Characteristics of chaotic masking in synchronized semiconductor lasers. *IEEE Journal of Quantum Electronics* **39**, 963-970 (2003).

[30] Uchida, A., Heil, T., Liu, Y., Davis, P. & Aida, T. High-frequency broad-band signal generation using a semiconductor laser with a chaotic optical injection. *IEEE Journal of Quantum Electronics* **39**, 1462-1467 (2003).

Figure captions

Figure 1: **Structure of random bit sequence generator using two chaotic lasers.**

a, Schematic diagram. **b**, Experimental setup. The lasers are the type used in optical fiber communications. They are semiconductor distributed-feedback (DFB) lasers, operating at 1.5 micrometer wavelength and generating around 1.5 mW of optical power. The lasers are modified to allow optical feedback from an external fiber reflector which reflects a fraction of the light back into the laser, inducing high-frequency chaotic oscillations of the optical intensity. The amplitude of the optical feedback can be adjusted by the variable fiber reflector. Polarization maintaining fibers are used for the optical fiber components. The intensity of the laser light output is converted to an electrical signal by a photodetector (12 GHz bandwidth) with AC coupling which removes the DC component, the signal is amplified by an electronic amplifier (18 dB gain, 20 GHz bandwidth) and then converted to a binary digital signal by a 1-bit ADC. The ADC consists of a comparator and a D flip flop, which first converts the input analog signal into a binary level by comparing with the threshold voltage, and then samples the binary level at the rising edge of an external clock. The two independent binary digital signals obtained from the two lasers are then combined by a XOR operation. The output signal from the XOR operation is a stream of bits with the format of Non-Return to Zero (NRZ) that is suitable for high-speed data communications. ADC, 1-bit analog-digital converter; Amp, electronic amplifier; F optical fiber; FC, fiber coupler; ISO, fiber isolator; OSC, digital oscilloscope; PD, photodetector; SL, semiconductor laser; Th_{1,2}, threshold voltages; VA variable fiber attenuator; VR, variable fiber reflector; XOR, Exclusive OR.

Figure 2: **Typical output signals from experimental system.**

a, Temporal waveforms of the laser outputs, the external clock, and the corresponding random bit sequence. **b**, Eye diagram of the random bit signal. **c**, Random bit patterns in two-dimensional plane. Bits 1 and 0 are converted into black and white dots, respectively, and placed from left to right (and from top to bottom). 500 by 500 bits are shown. The external cavity lengths in this case are set to 5.633 and 7.840 m for Laser 1 and 2, respectively, corresponding to feedback delay times (roundtrip) of 54.26 and 75.52 ns. The largest oscillation components of the two lasers, in the presence of optical feedback, are 3.07 and 2.86 GHz for Laser 1 and 2, respectively.

Figure 3: **Autocorrelation and spectral characteristics.**

a, Autocorrelation functions of the chaotic waveforms of the two lasers. τ_1 and τ_2 correspond to the feedback times of the external cavities. The values of $\tau_{1,2}$ can be controlled by adjusting the length of the external fiber cavity. τ_s , clock period. **b**, Enlargement of the short-time autocorrelation. τ_{c1} and τ_{c2} correspond to the largest component of the chaotic oscillation. The values of $\tau_{c1,c2}$ can be controlled by adjusting the injection current. τ_s , clock period. **c**, Autocorrelation function of random bit sequence output from the XOR device. One bit corresponds $\tau_s = 0.588$ ns ($1/\tau_s = 1.7$ GHz). The time scale of Fig. 3c corresponds to the time scale of Fig. 3a. It can be seen there is no autocorrelation corresponding to τ_1 , τ_2 , or any other delay. **d**, Radio-frequency spectra for the chaotic oscillation, laser noise, and photodetector-amplifier noise.

Table 1: Results of NIST Special Publication 800-22 statistical tests.

For “success” using 1000 samples of 1Mbit data and significance level $\alpha= 0.01$, the P-value (uniformity of p-values) should be larger than 0.0001 and the proportion should be in the range of 0.99 ± 0.0094392 . For the tests which produce multiple P-values and proportions, the worst case is shown.

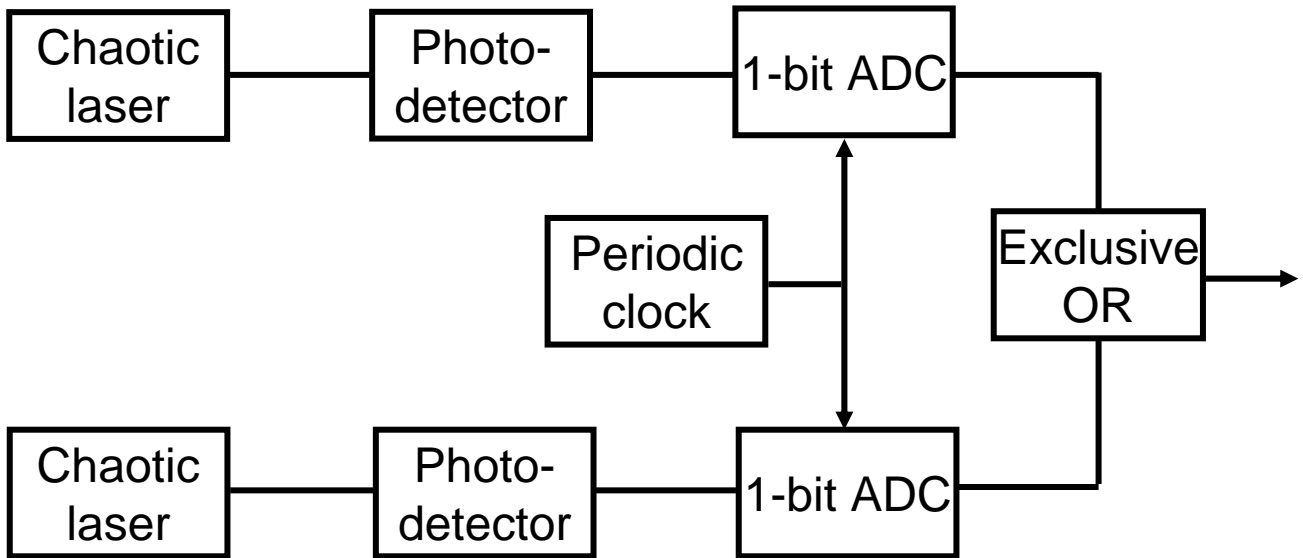


Fig.1a

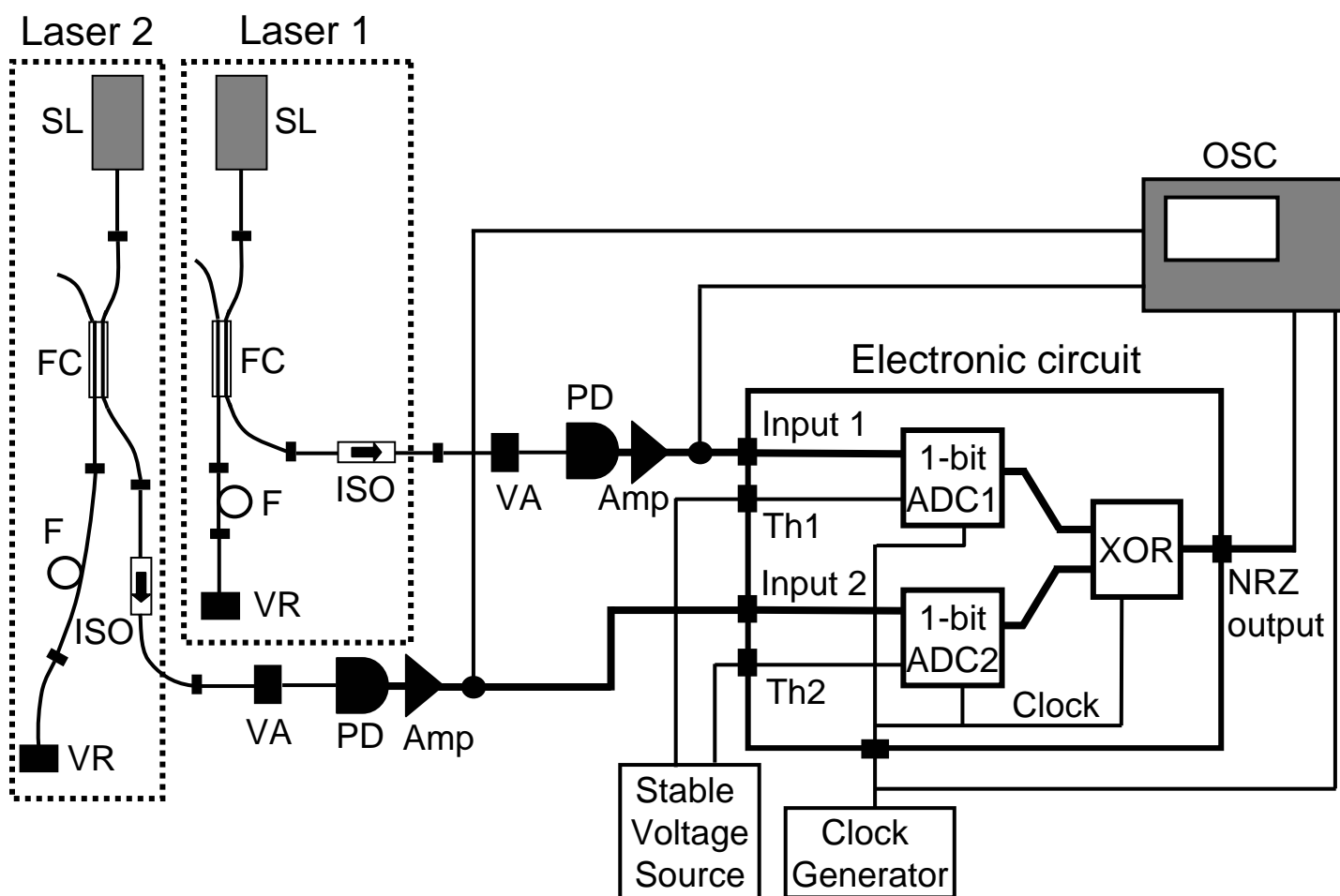


Fig.1b

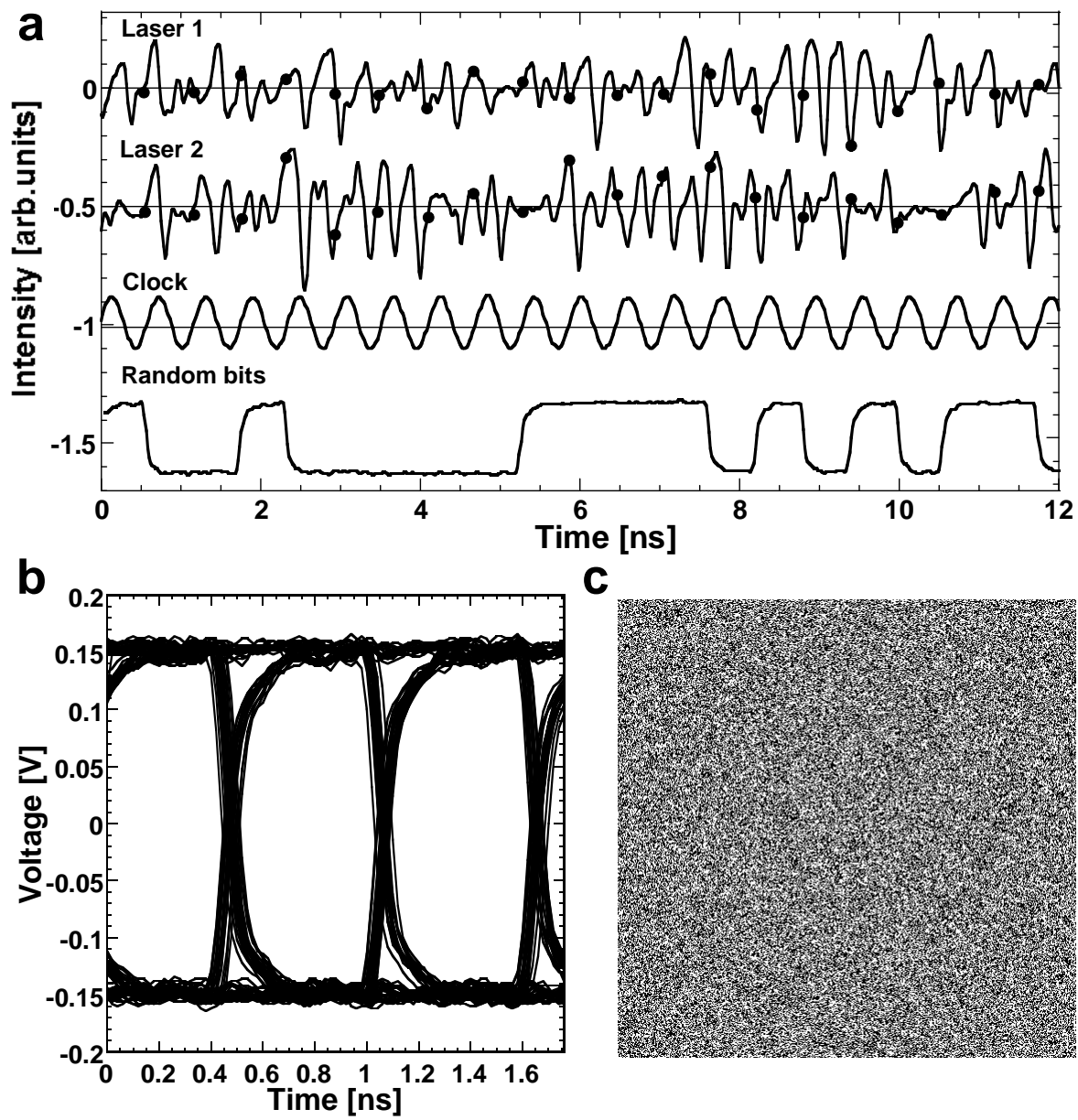


Fig.2

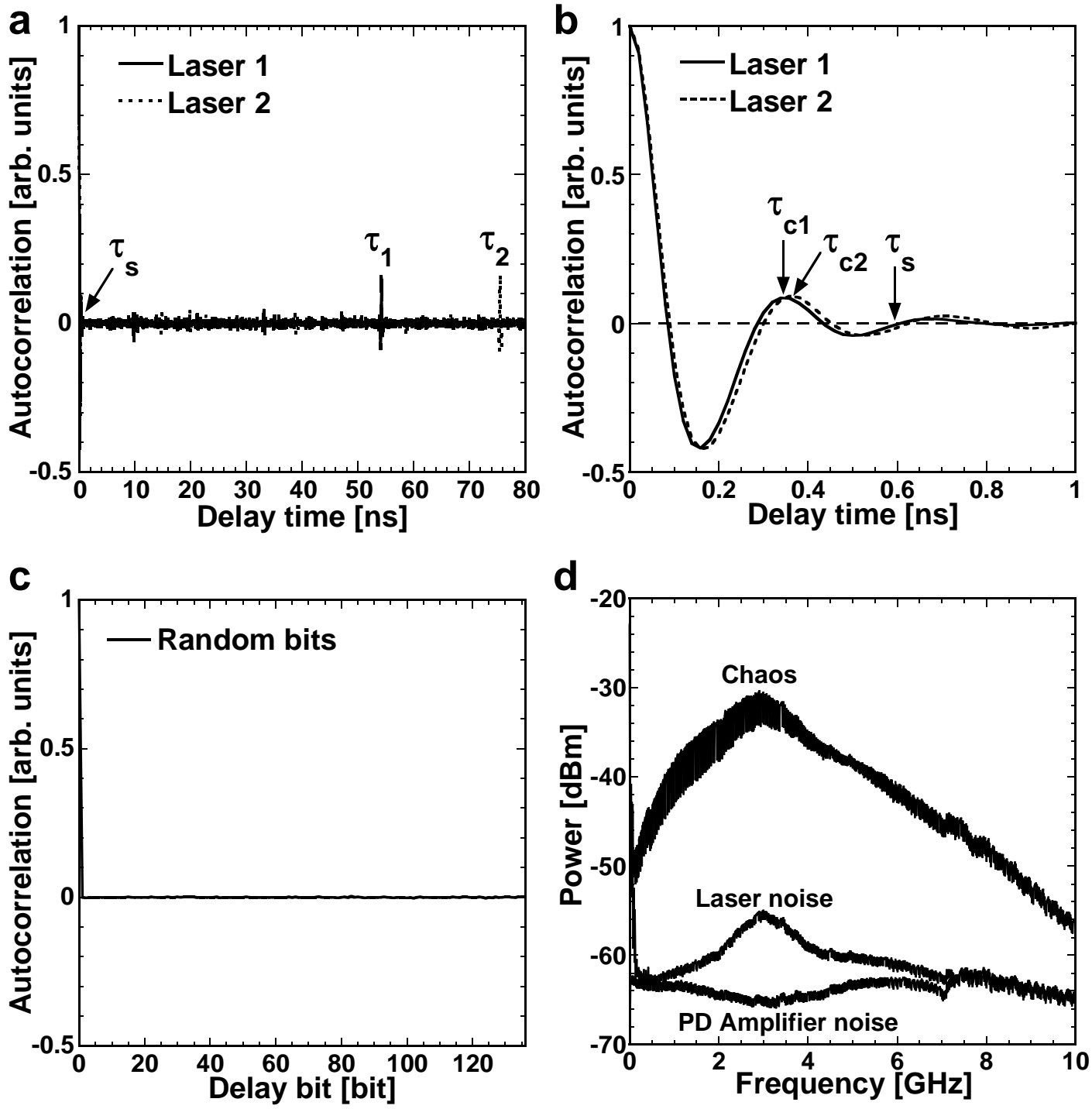


Fig.3

Table 1

| STATISTICAL TEST | P-VALUE | PROPORTION | RESULT |
|---------------------------|----------|------------|---------|
| frequency | 0.366918 | 0.9920 | SUCCESS |
| block-frequency | 0.639202 | 0.9900 | SUCCESS |
| cumulative-sums | 0.101311 | 0.9920 | SUCCESS |
| runs | 0.223648 | 0.9920 | SUCCESS |
| longest-run | 0.603841 | 0.9890 | SUCCESS |
| rank | 0.031012 | 0.9900 | SUCCESS |
| fft | 0.274341 | 0.9910 | SUCCESS |
| nonperiodic-templates | 0.013760 | 0.9810 | SUCCESS |
| overlapping-templates | 0.893482 | 0.9910 | SUCCESS |
| universal | 0.903338 | 0.9920 | SUCCESS |
| approximate-entropy | 0.880145 | 0.9920 | SUCCESS |
| random-excursions | 0.142248 | 0.9836 | SUCCESS |
| random-excursions-variant | 0.068964 | 0.9869 | SUCCESS |
| serial | 0.440975 | 0.9860 | SUCCESS |
| linear-complexity | 0.291091 | 0.9970 | SUCCESS |

Total

15

Supplementary Material

Supplementary Figure S1: **Details of laser system.**

a, Specifications of components. **b**, Conditions for laser chaos used to obtain data in Fig. 2.

Supplementary Figure S2: **Results of Diehard statistical test.**

For “success” for significance level $\alpha = 0.01$, the P-value (uniformity of p-values) should be larger than 0.0001. “KS” indicates that single P-value is obtained by the Kolmogorov-Smirnov (KS) test. For the tests which produce multiple P-values without KS test, the worst case is shown.

Supplementary Figure S3: **Divergence of chaotic oscillations due to laser noise.**

Numerical simulation of theoretical Lang-Kobayashi laser model with added noise showing significant divergence of trajectories after 1~2 ns. Simulation model is described in detail in Ref. [29]. The strength of added noise is adjusted to match the experimental noise power shown in Fig. 3d, which was obtained when the laser has no external optical feedback. **a**, Power spectrum of chaos and noise, corresponding to experimental result shown in Fig. 3d. **b**, An example of chaotic oscillation with and without added noise. **c**, Another example of chaotic oscillations with and without added noise.

Supplementary Figure S4: **Dependence of 0/1 ratio on threshold voltage for sequences generated with laser chaos and laser noise only.**

a, Percentage of occurrences of “1” bits for sequences generated using laser chaos. The slope value is 0.0256 % per mV. Good balance of “1” and “0” could be achieved with the threshold resolution of 0.1mV. **b**, Percentage of occurrences of “1” bits for sequences generated using laser noise only. The slope value is 5.241 % per mV. Good balance of “1” and “0” could NOT be achieved with the threshold resolution of 0.1mV.

Supplementary Video S1: Video of two-dimensional bit pattern shown in Fig. 2c.

Supplementary Figure S1: Details of laser system

(a) Specifications of components

| Component | Brand, Product ID, | Specifications |
|------------------|---|--|
| lasers | NTT Electronics, NLK1555CCA with fiber pigtail (no isolator) | optical wavelength: 1547 nm |
| laser controller | Newport, 8000-OPT-41-41-41-41 | |
| photodetectors | New Focus, 1554-B | bandwidth: 12 GHz |
| amplifiers | New Focus, 1422-LF | gain: 18dB bandwidth: 20 GHz |
| oscilloscope | Tektronix, DPO71254 | bandwidth: 12.5 GHz, sample rate: 50 Gsps |
| AD converter | prototype | input: AC couple bandwidth: 3 GHz output format: 0.3V (pp) NRZ threshold voltage: 0~100mV threshold resolution: 0.1mV |

(b) Conditions for laser chaos used to obtain data in Figs. 2 and 3

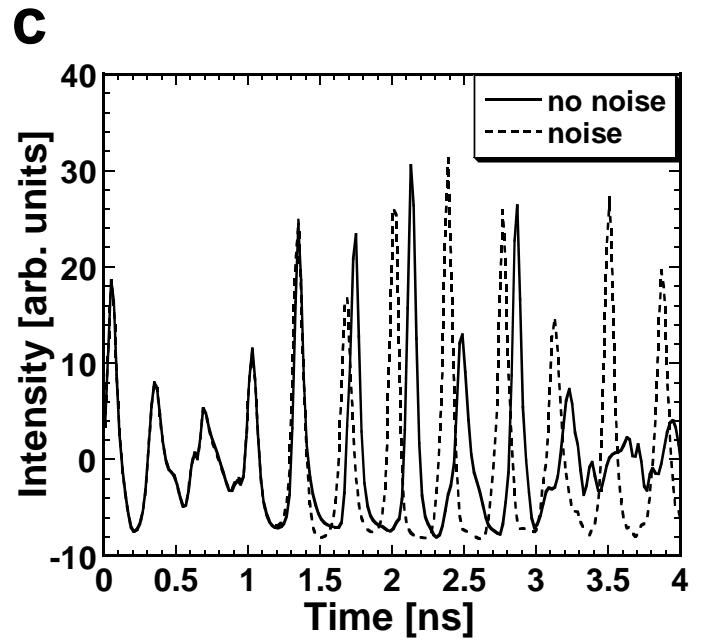
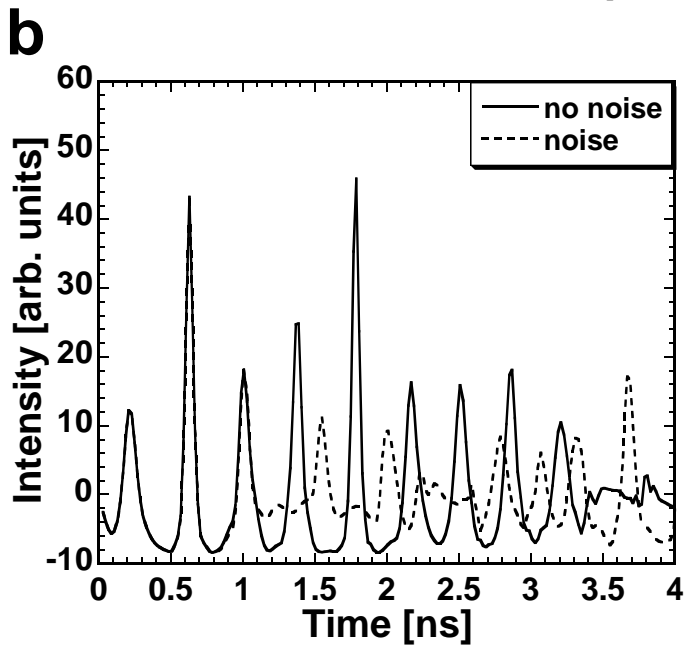
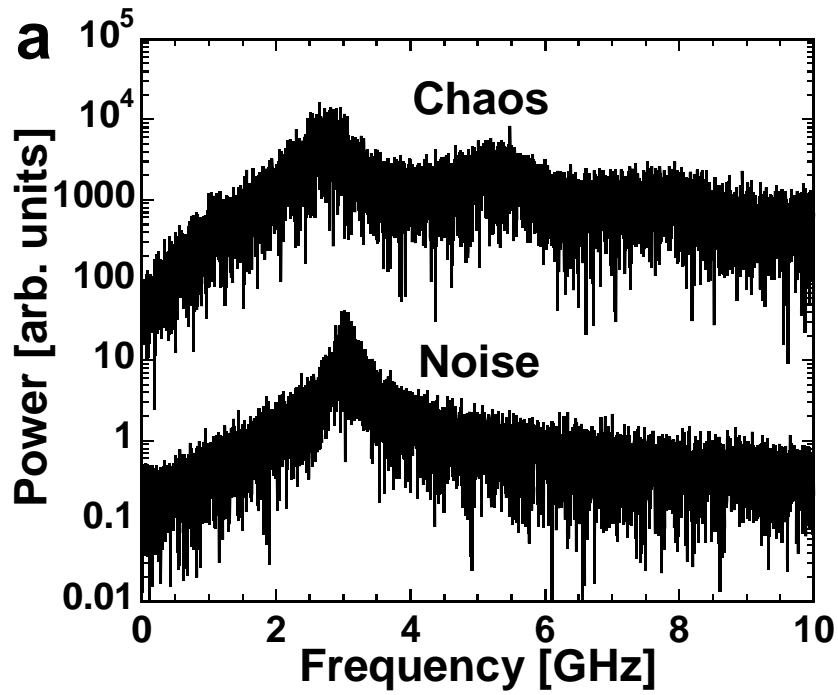
| Parameter | Laser 1 | Laser 2 |
|--|------------------------|------------------------|
| injection current (threshold injection current, I_{th}) | 16.05 mA (9.37 mA) | 15.72 mA (7.27 mA) |
| round-trip feedback delay time τ_1, τ_2 (external cavity length in fibers) | 54.26 ns (5.633 m) | 75.52 ns (7.840 m) |
| period of dominant oscillation component of chaos, τ_{c1}, τ_{c2} (dominant chaotic oscillation frequency) | 0.326 ns (3.07 GHz) | 0.350 ns (2.86 GHz) |
| Clock period τ_s (clock frequency) | 0.588 ns (1.70 GHz) | |

| STATISTICAL TEST | P-VALUE | RESULT | |
|---|----------|---------|----|
| birthday spacing | 0.493353 | SUCCESS | KS |
| overlapping 5-permutation | 0.860647 | SUCCESS | |
| binary rank for 31x31 matrices | 0.905862 | SUCCESS | |
| binary rank for 32x32 matrices | 0.324578 | SUCCESS | |
| binary rank for 6x8 matrices | 0.026400 | SUCCESS | KS |
| bitstream | 0.019300 | SUCCESS | |
| Overlapping-Pairs-Sparse-Occupancy | 0.035000 | SUCCESS | |
| Overlapping-Quadruples-Sparse-Occupancy | 0.096900 | SUCCESS | |
| DNA | 0.013200 | SUCCESS | |
| count-the-1's on a stream of bytes | 0.650262 | SUCCESS | |
| count-the-1's for specific bytes | 0.079061 | SUCCESS | |
| parking lot | 0.231274 | SUCCESS | KS |
| minimum distance | 0.770625 | SUCCESS | KS |
| 3D spheres | 0.883907 | SUCCESS | KS |
| squeeze | 0.717981 | SUCCESS | |
| overlapping sums | 0.702774 | SUCCESS | KS |
| runs | 0.252852 | SUCCESS | KS |
| craps | 0.150910 | SUCCESS | |

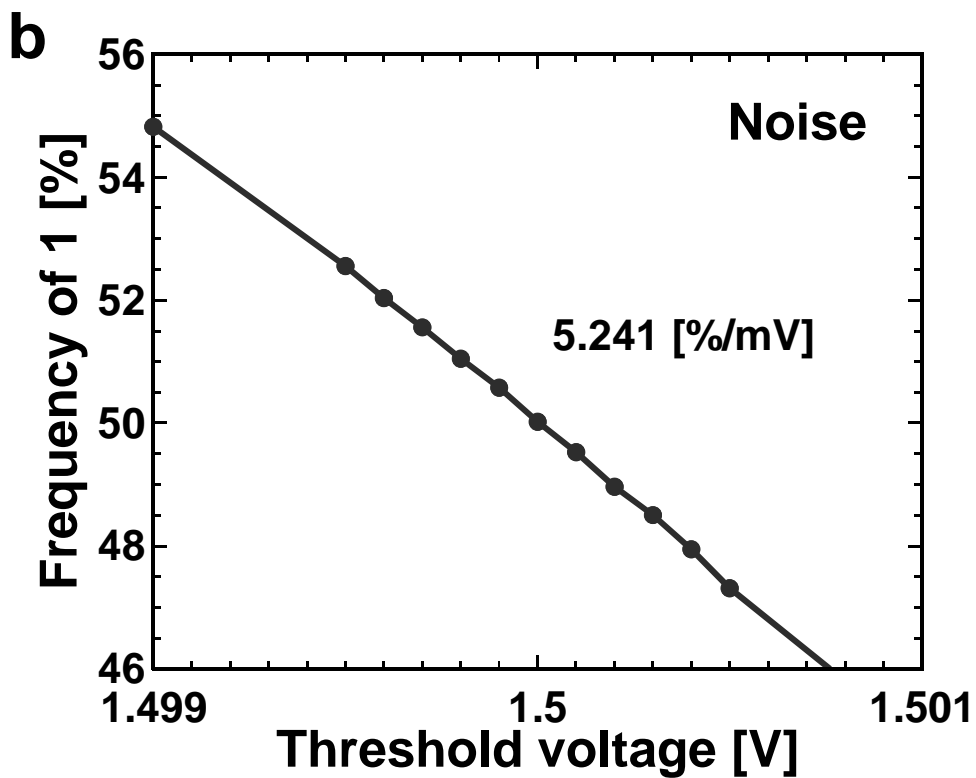
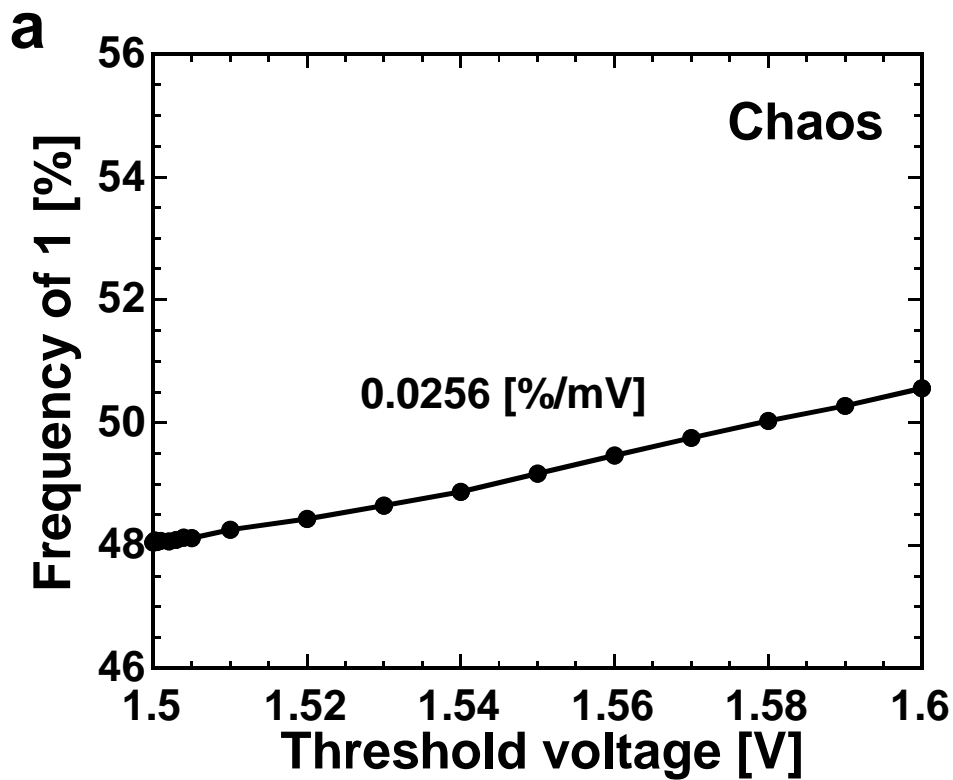
Total

18

Supplementary Figure S2



Supplementary Figure S3



Supplementary Figure S4